Single-wall-carbon-nanotube/single-carbon-chain molecular junctions

Felix Börrnert,[1,*] Carina Börrnert,[2] Sandeep Gorantla,[1] Xianjie Liu,[3] Alicja Bachmatiuk,[1] Jan-Ole Joswig,[4] Frank R. Wagner,[2] Franziska Schäffel,[1] Jamie H. Warner,[5] Ronny Schönfelder,[1] Bernd Rellinghaus,[1] Thomas Gemming,[1] Jürgen Thomas,[1] Martin Knupfer,[1] Bernd Büchner,[1] and Mark H. Rümmeli[1,4,†]

[1]*Leibniz-Institut für Festkörper- und Werkstoffforschung Dresden e. V., PF 27 01 16, 01171 Dresden, Germany*

[2]*Max-Planck-Institut für Chemische Physik fester Stoffe, Nöthnitzer Straße 40, 01187 Dresden, Germany*

[3]*Linköpings Universitet, 581 83 Linköping, Sweden*

[4]*Technische Universität Dresden, 01062 Dresden, Germany*

[5]*University of Oxford, Parks Rd., Oxford, OX1 3PH, United Kingdom*

(Received 21 December 2009; revised manuscript received 3 February 2010; published 24 February 2010; corrected 1 March 2010)

Stable junctions between a single carbon chain and two single-wall carbon nanotubes were produced via coalescence of functionalized fullerenes filled into a single-wall carbon nanotube and directly imaged by *in situ* transmission electron microscopy. First principles quantum chemical calculations support the observed stability of such molecular junctions. They also show that short carbon chains bound to other carbon structures are cumulenes and stable semiconductors due to Peierls-like distortion. Junctions like this can be regarded as archetypical building blocks for all-carbon molecular electronics.

DOI: 10.1103/PhysRevB.81.085439 PACS number(s): 61.48.De, 82.37.−j

I. INTRODUCTION

In the design of nanoelectronic devices, a key issue is the fabrication of metal–semiconductor junctions.[1] A single molecular junction between a single carbon chain (SCC) and a single-wall carbon nanotube (SWNT) could provide an attractive solution. Whether a SWNT is semiconducting or metallic is controlled either through its chirality or through doping.[2,3] Several theoretical works have explored the transport properties of a SCC.[4–10] Infinite SCCs are semiconducting due to Peierls distortion.[11] However, short SCCs are usually treated as metallic in the literature. Single carbon chains have previously been observed.[12–14] However, the methods used are not best suited for the large scale production of SCCs and do not form controllable junctions.

In this study, we present an elegant solution to provide excess carbon material to SWNTs through utilization of surface functionalized fullerenes filled into a host SWNT and the tendency of the filling fullerenes to coalesce when heated is exploited to form an inner SWNT with ligands attached.[15,16] Appropriate molecular species attached to the fullerenes can then serve as building blocks for carbon chains. Time series aberration-corrected low-voltage high-resolution transmission electron microscopy (TEM) is used as a suitable tool to directly observe the dynamics of the reaction.[17] Quantum chemical calculations are performed using several model systems under different environmental conditions to gain insight into the thermal stability of the junction and the electronic structure of the SCC. In contrast to previous reports we find that the carbon chain is a stable semiconductor.

II. EXPERIMENTAL

Here, SWNTs filled with [6,6]-phenyl-C_{61}-butyric-acid-methyl-ester (PCBM) are used.[18] The SWNTs employed were produced by a laser ablation route and have a mean diameter of 1.5 nm.[19] They were opened by annealing in air at 380 °C for 0.5 h and filled with PCBM by annealing both the SWNTs and the PCBM together in a sealed quartz ampule with an internal pressure of 10^{-3} Pa at 550 °C for 5 days.

Infrared absorption spectra were taken with the as-produced sample pressed on KBr crystals using a Bruker IFS 113v Fourier transform spectrometer. A FEI Titan^3 80–300 transmission electron microscope with a CEOS aberration corrector for the objective lens, operating at an acceleration voltage of 80 kV, equipped with a Gatan UltraScan 1000 camera was used. During a time series an image was taken every 5 s with an acquisition time of 0.5 s and all images were compiled into motion pictures.[20] The contrast of the micrographs was enhanced through Fourier filtering. The chirality of the SWNTs was determined by analyzing the Fourier transformed TEM images and measuring the corrected SWNT diameter.[17] Simulations of the imaging process were obtained using JEMS electron microscopy software.[21] For comparison, noise was added to the simulated images and the same Fourier filtering as for the TEM images was applied.

Born-Oppenheimer molecular-dynamics (MD) simulations[22,23] employed a density-functional tight-binding method as implemented in the deMon code.[24] The trajectories have been obtained with a time-step of 0.02 fs (1500–2000 K), 0.05 fs (700–1000 K) and 0.1 fs (300 K) and a local Berendsen thermostat. Before studying the temperature dependent behavior of the system, the start geometry was equilibrated at 300 K. The temperature-dependent calculations were performed after an equilibration period at the particular temperature. The dwell of the simulations was 20 ps. To ensure the stability of the model at 1000 K, this calculation was restarted for further 40 ps.

First principles density-functional theory (DFT) based calculations were performed using the PBE exchange-correlation functionals as implemented in the Gaussian code.[25,26] Electron localizability indicator (ELI-D)[27] and delocalization index[28] were calculated using the DGRID code.[29] For the details of the DFT calculations see Ref. 20.

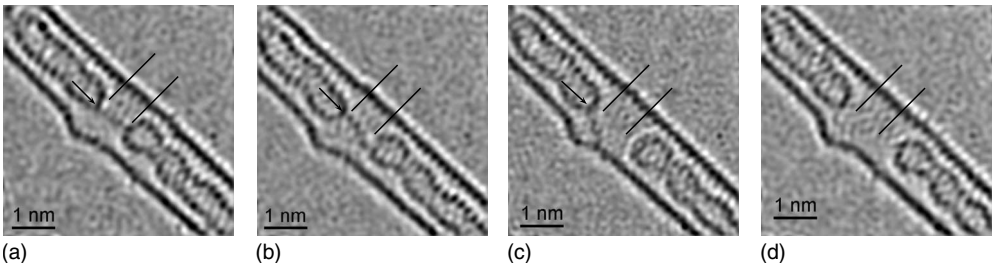

FIG. 1. *In situ* study showing the dynamics of a SCC bridging two SWNTs inside a host tube. (a) SCC bridging the two inner tubes. The attachment of the SCC to the upper inner tube is indicated by an arrow, and the distance between the inner tube sections represented by two bars, (b) the attachment point of the SCC to the upper tube has changed. (c) The chain disconnects from the lower inner tube. The two inner tubes drift apart, and (d) the SCC disappears and the inner tube sections drift further apart. The time elapsed from image (a) to (d) is 30 s.

III. RESULTS

A. *In situ* TEM study

In Fig. 1(a) the capped ends from two inner SWNTs with a chain bridging them can be seen. The host SWNT features a distortion in the wall structure. The inner SWNTs were formed earlier via the coalescence of PCBM fullerenes driven by the electron beam (see Fig. 2).[16] In Fig. 1(b), the chain binding the two inner tubes appears to have altered its position [see arrows in frames (a) and (b)]. This apparent change in the attachment point could be due to the chain anchor point being mobile or the upper inner tube has rotated. However, the rotation argument is unlikely, because in Fig. 1(c) the attachment point of the chain to the upper inner tube has again changed, yet the upper inner tube structure remained. In frame (c) one can also observe that the chain has now disconnected from the lower inner tube and the spacing between the two inner tubes has clearly augmented (the markers indicate the spacing found in frame (a) across all frames), suggesting the SCC may have been under strain. The detached end of the chain is seen to have found a new anchor point at the humplike feature on the host tube. One can anticipate this distortion to be a reactive region since added leads to enhanced chemical reactivity.[30] In Fig. 1(d) the two inner SWNTs have drifted apart further and the carbon chain has disappeared. The humplike structure on the host tube appears slightly larger suggesting the carbon chain has been absorbed within it. However, it may be possible that part or all of the carbon chain was ejected from the host tube altogether.[31]

To better comprehend the carbon chain bridging the two SWNTs within a host tube we generated various simulations of the structure imaging process, see Fig. 3. A section of the structure from the original micrograph is provided in frame (a). In frame (b) we present the result of an imaging simulation which matches the original image. The complete underlying ball-and-stick structure is provided in panel (c) from which one can see where regions of strong contrast originate. In panel (d) the ball-and-stick structure of the carbon chain bridging the two SWNTs without the host tube is presented. The chirality of the host tube is (14,8). While one cannot conclusively determine the chirality of the inner SWNT since they are probably still rearranging their structure; our best fit

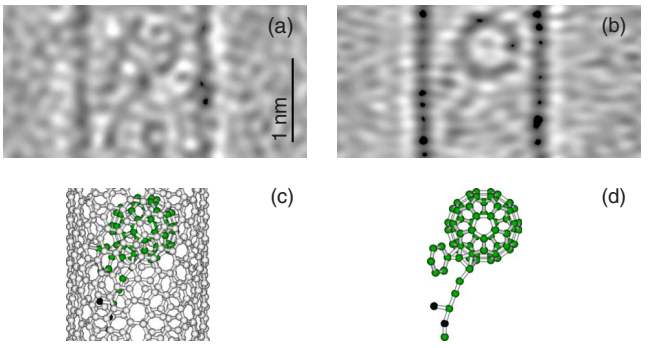

FIG. 2. (Color online) Comparison of original and simulation of a TEM image of the PCBM molecule filled into a SWNT using molecular models. (a) Fourier filtered original TEM image showing a PCBM molecule residing in a host SWNT, (b) Fourier filtered output of a multislice simulation of the imaging process, (c) ball-and-stick illustration of the underlying molecular model for the simulation, hydrogen atoms are omitted for clarity, and (d) ball-and-stick illustration of the inner part of the underlying molecular model. (Simulation parameters: Accelerating voltage 80 kV, chromatic aberration 1.1 mm, spherical aberration 0.002 mm, defocus 2 nm, energy spread 0.8 eV, defocus spread 9 nm, noise 2%.)

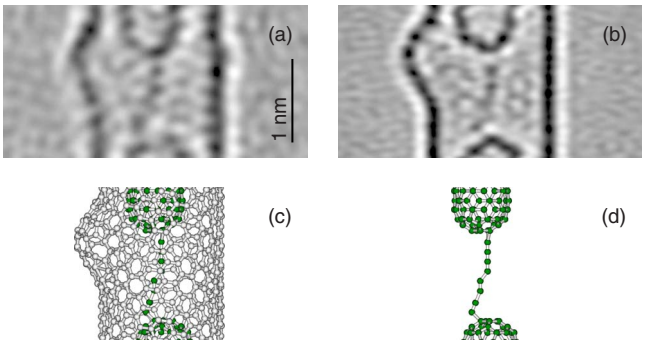

FIG. 3. (Color online) Comparison of original and simulation of a TEM image of the SWNT/SCC molecular junction using molecular models. (a) Fourier filtered TEM image [cut from Fig. 1(b)], (b) Fourier filtered output of a multi-slice simulation of the imaging process, (c) ball-and-stick illustration of the underlying molecular model for the simulation, and (d) of the inner part of the model to highlight the single carbon chain. (Simulation parameters: Accelerating voltage 80 kV, chromatic aberration 1.1 mm, spherical aberration 0.002 mm, defocus 7 nm, energy spread 0.8 eV, defocus spread 9 nm, noise 2%.)

is a (5,5) for both tubes. The carbon chain length is 8 atoms (see below).

Infrared absorption studies on PCBM filled SWNTs annealed under dynamic ultrahigh vacuum (UHV) conditions at 1500 K show no C–H vibrations confirming cumulene structures are likely, as opposed to alkane chain or polyacetylene-type structures. In addition, the stability of the SWNT/SCC molecular junction we observed was high; it withstood the energy input of the electron beam for over 30 s. Compared to other carbon structures under similar conditions, this value is remarkably high.[32] This stability indicates the carbon chain is most probably entirely formed from carbon atoms as the incorporation of an O or H atom would make it unstable.[33] A stable carbon chain bridging carbon nanotubes is potentially attractive as a molecular electronic device. In this case it would need to be freed from the confines of the host tube (nanoreactor), say by "unzipping" the host tube.[34,35]

To further investigate the electronic properties and stability of a carbon chain bridging two SWNTs, various first principles quantum chemical calculations were performed.

B. MD simulations

The MD simulations were performed on a model consisting of an eight-atom carbon chain with two C_{60} fullerenes at each end mimicking the inner SWNT caps. Experimentally, the coalescence of fullerenes is accomplished by annealing in UHV at a temperature of 1500 K.[36] Hence the MD simulations were performed from 300 K up to 2000 K. The attachment point of the chain to the fullerene was calculated either bridging the common bond of two hexagons ([6,6]) or that of a hexagon and a pentagon ([5,6]). In all simulations the bridging bond is cracked (2.125 Å at 300 K) and an annulene type segment is formed. Energetically, there is no preference between these two bridging configurations.

The model is stable up to a temperature of 1000 K. For higher temperatures the chain disconnects from the fullerenes irreversibly as we observe experimentally. The initial step is induced by the breathinglike contraction of the fullerene at high temperatures. For simulations at 2000 K a subsequent separation from both fullerenes was observed in a time scale of 20 ps, resulting in two fullerenes and a stable isolated carbon chain. The MD simulations do not show any movement at the attachment point as observed in the TEM studies. A movement of the anchor points would not be expected because of the weak delocalization of the double bonds in fullerenes. This suggests the SCC/SWNT junction movement is due to the electron beam irradiation. The presence of the host tube in the experimentally observed system should not affect the mechanical stability of the junction, because the effect of mechanisms like charge transfer on the covalent bond strength are weak.

Cumulene systems (see below) are usually considered to be straight, nevertheless, deformations down to 120° (2000 K) are tolerated by the model [see Fig. 4(c)]. A decrease in the average mean angle from about 168° (300 K) down to 153° (2000 K) is obtained, while the angle distribution is broadened with increasing temperature. The bond lengths in the carbon chain averaged over all trajectories alternate reflecting a Peierls-like distortion (Table I). In Fig. 4(b) it is shown that the magnitude of the bond length alternation is independent of the temperature.

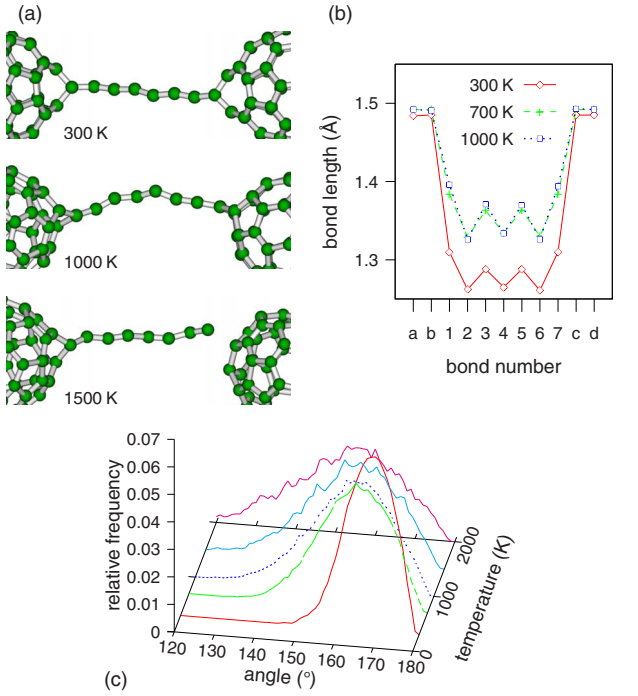

FIG. 4. (Color online) MD simulations of the chain. (a) Snapshots from simulations at 300 K, 1000 K, and 1500 K. (b) Bond lengths averaged over all MD trajectories at 300, 700, and 1000 K [for bond numbers see Fig. 5(b)]. (c) Temperature dependent angle distribution in the carbon chain.

C. First principles DFT calculations

The MD simulations were complemented using first principles DFT calculations. Different geometry optimized model systems were evaluated and single-point calculations on two MD snapshots of distorted chains were conducted. The geometry optimizations are done for an eight-atom carbon chain saturated with either four hydrogen atoms or two 1,6-methano[10]annulene groups imitating the tube ends. The geometry optimized models converge into stable chains with a length of 9 Å from C^1 to C^8 and alternating bonds lengths similar to those of the MD simulations. The electronic structure of the chain was studied in position space by means of the topological analysis of the calculated ELI-D and by calculating the delocalization index δ between the atomic basins of the electron density. For the optimized geometries an energy gap of 2 eV was obtained. The C–C delocalization index within the geometry optimized chains alternates between 1.92 and 1.61 and is only affected by the substituted groups for the first and the last bond in the chain. Adjacent ELI-D iso-surfaces, that each consist of two ELI-D maxima, stand perpendicularly with respect to each other [see Fig. 5(b)]. Both the delocalization indices and the ELI-D signatures indicate a bond order of two for each bond within the chain, thereby, implying a cumulene structure. A deformation of the chain is tolerated initially [see Fig. 5(b)]. The

TABLE I. Bond lengths, delocalization indices, and highest occupied molecular orbital-lowest unoccupied molecular orbital (HOMO–LUMO) gap of the carbon chain [for bond numbering see Fig. 5(b)].

Bond number	a	b	1	2	3	4	5	6	7	c	d	
						Bond length (Å)						HOMO–LUMO gap (eV)
DFT optimized R=H	1.093	1.093	1.322	1.274	1.291	1.276	1.291	1.274	1.322	1.093	1.093	2.03
DFT optimized R=$C_{10}H_8$	1.478	1.478	1.330	1.284	1.301	1.287	1.301	1.284	1.330	1.478	1.478	1.93
MD snapshot 300 K	1.434	1.466	1.369	1.277	1.328	1.274	1.332	1.251	1.359	1.482	1.461	1.50
MD snapshot 2000 K	1.451	1.553	1.487	1.323	1.312	1.281	1.448	1.233	1.437	1.476	1.478	1.09
averaged over MD trajectories 300 K	1.485	1.484	1.310	1.262	1.288	1.265	1.288	1.261	1.310	1.485	1.485	
averaged over MD trajectories 1000 K	1.492	1.491	1.396	1.326	1.371	1.334	1.370	1.326	1.394	1.493	1.491	
						Delocalization index						
DFT optimized R=H	0.93	0.93	1.72	1.92	1.75	1.87	1.76	1.92	1.72	0.93	0.93	
DFT optimized R=$C_{10}H_8$	0.98	0.98	1.61	1.92	1.75	1.87	1.75	1.92	1.61	0.98	0.98	
MD snapshot 300 K	1.04	1.01	1.53	1.98	1.66	1.88	1.61	2.01	1.56	1.00	1.02	
MD snapshot 2000 K	1.04	0.88	1.44	1.95	1.63	2.02	1.49	2.10	1.34	1.03	1.06	

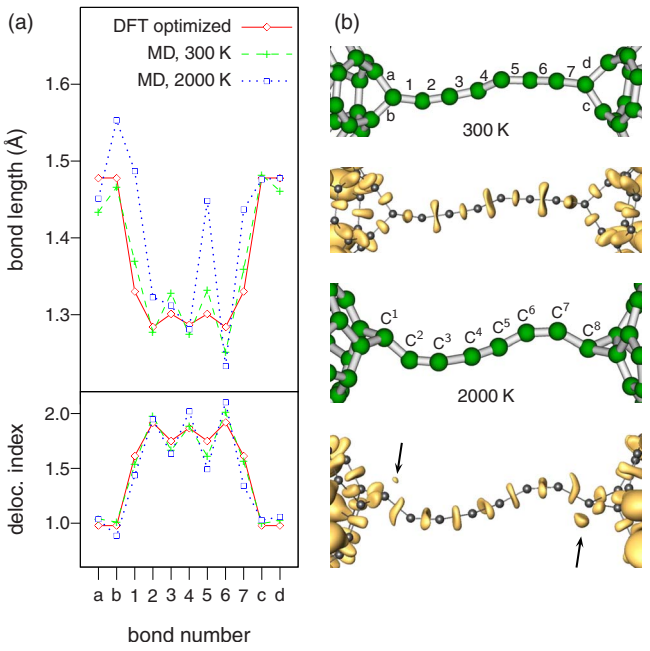

FIG. 5. (Color online) DFT calculations with delocalization index and ELI-D evaluation of the chain. (a) top panel—bond lengths between the single atoms of the chain taken from a DFT optimized geometry and snapshots from MD simulations at 300 K and 2000 K [see panels (b) and (c)], bottom panel—delocalization index, (b) MD simulation snapshot (top) and corresponding isosurfaces (bottom) from ELI-D calculations. MD simulation at a temperature of 300 K with maximum distortion, the bond numbers are indicated, the topology of the isosurfaces is similar to the optimized case. (c) 2000 K simulation with the atoms labeled, with characteristic ELI-D isosurfaces visualizing a cumulene structure type for each model, and additional electron localizability maxima perpendicular above carbon sites C^1 and C^8 (arrows).

two bonding indicators show no qualitative change in the bonding condition. However, significant changes emerge with strong deformation of the chain as seen in Fig. 5(c). Additional electron localizability maxima can be seen above the terminating carbon atoms of the chain (C^1,C^8). These are centers of increased reactivity. Furthermore, it can be seen from Fig. 5(a), that the δ from a single bond b connecting the carbon chain with the substituent decreases, whereas the bond length is increased. This describes a successive bond breaking mechanism at the junctions in full agreement with our experimental observations.

IV. CONCLUSIONS

We have introduced a novel method to produce single-carbon-chain/single-wall-carbon-nanotube (SCC/SWNT) molecular junctions. *In situ* aberration-corrected low-voltage transmission electron microscopy observations show the dynamics of a single carbon chain bridging two SWNTs. Density functional theory based calculations indicate that the SCC/SWNT junction is stable up to 1000 K. Electron localizability indicator and delocalization index bond analysis clearly reveals a cumulene bond type. A Peierls-distortion-like structure is evidenced for short carbon chains connected to other structures. This induces an energy gap making short carbon chains highly suitable as nanosized semiconductor devices. A single carbon chain connected to two metallic SWNTs, as shown here, could provide the foundations for remarkably small field effect transistors.

ACKNOWLEDGMENTS

We thank R. Hübel and S. Leger for technical support. C.B. acknowledges the CNV-Stiftung, S.G. the "Pakt für Forschung und Innovation," F.S. the Cusanuswerk, and M.H.R. the EU (ECEMP) and the Freistaat Sachsen.

*f.boerrnert@ifw-dresden.de
†m.ruemmeli@ifw-dresden.de

[1] C. Joachim, J. K. Gimzewski, and A. Aviram, Nature (London) **408**, 541 (2000).
[2] S. Kazaoui, N. Minami, R. Jacquemin, H. Kataura, and Y. Achiba, Phys. Rev. B **60**, 13339 (1999).
[3] S. Latil, S. Roche, D. Mayou, and J.-C. Charlier, Phys. Rev. Lett. **92**, 256805 (2004).
[4] N. D. Lang and P. Avouris, Phys. Rev. Lett. **81**, 3515 (1998).
[5] N. D. Lang and P. Avouris, Phys. Rev. Lett. **84**, 358 (2000).
[6] B. Larade, J. Taylor, H. Mehrez, and H. Guo, Phys. Rev. B **64**, 075420 (2001).
[7] S. Tongay, R. Senger, S. Dag, and S. Ciraci, Phys. Rev. Lett. **93**, 136404 (2004).
[8] V. V. Ivanovskaya, N. Ranjan, T. Heine, G. Merino, and G. Seifert, Small **1**, 399 (2005).
[9] H. J. Choi, M. L. Cohen, and S. G. Louie, Phys. Rev. B **76**, 155420 (2007).
[10] K. H. Khoo, J. B. Neaton, Y. W. Son, M. L. Cohen, and S. G. Louie, Nano Lett. **8**, 2900 (2008).
[11] A. Abdurahman, A. Shukla, and M. Dolg, Phys. Rev. B **65**, 115106 (2002).
[12] H. E. Troiani, M. Miki-Yoshida, G. A. Camacho-Bragado, M. A. L. Marques, A. Rubio, J. A. Ascencio, and M. Jose-Yacaman, Nano Lett. **3**, 751 (2003).
[13] C. Jin, H. Lan, L. Peng, K. Suenaga, and S. Iijima, Phys. Rev. Lett. **102**, 205501 (2009).
[14] T. D. Yuzvinsky, W. Mickelson, S. Aloni, G. E. Begtrup, A. Kis, and A. Zettl, Nano Lett. **6**, 2718 (2006).
[15] B. W. Smith, M. Monthioux, and D. E. Luzzi, Nature (London) **396**, 323 (1998).
[16] J. H. Warner, Y. Ito, M. H. Rümmeli, T. Gemming, B. Büchner, H. Shinohara, and G. A. D. Briggs, Phys. Rev. Lett. **102**, 195504 (2009).
[17] A. Hashimoto, K. Suenaga, A. Gloter, K. Urita, and S. Iijima, Nature (London) **430**, 870 (2004).
[18] J. C. Hummelen, B. W. Knight, F. LePeq, F. Wudl, J. Yao, and C. L. Wilkins, J. Org. Chem. **60**, 532 (1995).
[19] M. H. Rümmeli, C. Kramberger, M. Löffler, O. Jost, M. Bystrzejewski, A. Grüneis, T. Gemming, W. Pompe, B. Büchner, and T. Pichler, J. Phys. Chem. B **111**, 8234 (2007).
[20] See supplementary material at http://link.aps.org/supplemental/10.1103/PhysRevB.81.085439 for (details of the DFT calculations).
[21] P. A. Stadelmann, Ultramicroscopy **21**, 131 (1987).
[22] D. Porezag, T. Frauenheim, T. Köhler, G. Seifert, and R. Kaschner, Phys. Rev. B **51**, 12947 (1995).
[23] G. Seifert, D. Porezag, and T. Frauenheim, Int. J. Quantum Chem. **58**, 185 (1996).
[24] A. M. Köster *et al.*, *deMon2k*, deMon developers (2006).
[25] M. J. Frisch *et al.*, *Gaussian 03*, Gaussian, Inc. (2004).
[26] J. P. Perdew, K. Burke, and M. Ernzerhof, Phys. Rev. Lett. **77**, 3865 (1996).
[27] M. Kohout, Int. J. Quantum Chem. **97**, 651 (2004).
[28] R. F. W. Bader and M. E. Stephens, J. Am. Chem. Soc. **97**, 7391 (1975).
[29] M. Kohout, *DGrid 4.5* (2009).
[30] R. C. Haddon, Science **261**, 1545 (1993).
[31] F. Börrnert *et al.* (unpublished).
[32] J. H. Warner, F. Schäffel, G. Zhong, M. H. Rümmeli, B. Büchner, J. Robertson, and G. A. D. Briggs, ACS Nano **3**, 1557 (2009).
[33] T. D. Yuzvinsky, A. M. Fennimore, W. Mickelson, C. Esquivias, and A. Zettl, Appl. Phys. Lett. **86**, 053109 (2005).
[34] D. V. Kosynkin, A. L. Higginbotham, A. Sinitskii, J. R. Lomeda, A. Dimiev, B. K. Price, and J. M. Tour, Nature (London) **458**, 872 (2009).
[35] L. Jiao, L. Zhang, X. Wang, G. Diankov, and H. Dai, Nature (London) **458**, 877 (2009).
[36] S. Bandow, M. Takizawa, K. Hirahara, M. Yudasaka, and S. Iijima, Chem. Phys. Lett. **337**, 48 (2001).